http://pubs.acs.org/journal/acsodf

Article

Research on Properties of Silicone-Modified Epoxy Resin and 3D Printing Materials

Zhen-Guo Yan, Zhen-Ping Wang, Ying-Ying Liu, Yang Xiao,* and Ning Yue

Cite This: *ACS Omega* 2023, 8, 23044−23050

ABSTRACT: A kind of organosilicon intermediate was prepared using isophorone diisocyanate (IPDI), hydroxyl silicone oil (HSO), and hydroxyethyl acrylate (HEA). The organosilicon modification of epoxy resin was realized by introducing a −Si−O− group into the side chain of epoxy resin by chemical grafting. The effects of organosilicon modification of epoxy resin on the mechanical properties systematically discuss its heat resistance and micromorphology. The results indicate that the curing shrinkage of the resin was decreased and the printing accuracy was improved. At the same time, the mechanical properties of the material are enhanced; the IS and elongation at break (EAB) are enhanced by 32.8 and 8.65%, respectively. The brittle fracture is changed to a ductile fracture, and the tensile strength (TS) of the material is decreased. The glass transition temperature (GTT) of the modified epoxy resin increased by 8.46 °C, and $T_{50\%}$ and T_{max} increased by 1.9 and 6 °C, respectively, indicating that the heat resistance of the modified epoxy resin was improved.

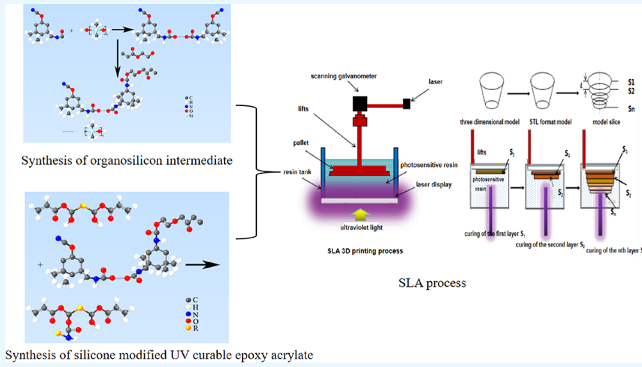

1. INTRODUCTION

3D printing is a new revolution in the world for the manufacturing field. It can reach high complexity and precision of the structure that traditional manufacturing cannot and has a unique manufacturing concept in die-free forming.[1−3] SLA technology has the highest precision in the 3D printing field at present.[4−7] An SLA-3D electron beam initiated polymerization on a layer of resin or monomer solution. The monomer quickly changed into a polymer chain after activation. After polymerization, only the needed parts were solidified in the resin layer. The material of SLA is a kind of liquid resin; it can be rapidly transformed from liquid resin to solid resin under UV light. This process can lead to the shrinkage of material volume, and too large volume shrinkage affects the forming accuracy and properties of the material, which makes it difficult to meet the application demand. Epoxy resin is widely used in various fields due to its excellent properties,[8−12] including SLA-3D, but it has the disadvantages of high curing shrinkage, poor toughness, poor heat resistance, and low precision of molding parts, which make it difficult to meet the application requirements.[13−17] Organosilicon, as a material with good thermal stability, oxidation resistance, weather resistance, and low temperature properties, can make up for the defects of epoxy resin to some extent.[18−21] At present, most of the research studies on silicone-modified epoxy resin are that the amino group and halogen atom in silicone are used to open the ring with the epoxy group.[22−25] Although the epoxy resin has been modified successfully, the curing performance has also been improved, but it causes the consumption of the epoxy group, so the crosslinking density of the system is reduced; thus, the glass conversion temperature of the resin is reduced.[26−31] Therefore, it is of great significance to investigate the toughening and reinforcing of epoxy resin, improving the mechanical properties and the precision of the molding parts. Based on this, the paper selects bisphenol, an epoxy acrylate, as the matrix and uses chemical grafting to study the heat resistance, mechanical properties, and micromorphology of the modified epoxy resin.

In this work, a kind of intermediate organosilicon product was prepared by using bisphenol, an epoxy acrylic acid, as the matrix using isophorone diisocyanate (hereinafter referred to as IPDI), hydroxysilicone oil, and hydroxyethyl acrylate (hereinafter referred to as HEA) as raw materials, and the matrix was modified. The isocyanate of the intermediate product reacting to the hydroxyl group of the epoxy resin was researched, and the effects of the 3D printing system under different n(silicone):n(EA) mole ratios on the GTT, viscosity, thermal stability, shrinkage, EAB, TS, IS, and hardness of the modified epoxy were discussed.

Received: April 4, 2023
Accepted: May 31, 2023
Published: June 14, 2023

https://doi.org/10.1021/acsomega.3c02275
ACS Omega 2023, 8, 23044−23050

2. RESULTS AND DISCUSSION

2.1. Determination of the −NCO Value. During the reaction, 0.1 g sample was weighed and put into a 50 mL plug conical flask, then 20 mL of 0.1 mol/L acetone di-*n*-butylamine solution was added, the plug was closed, and the stirring time was 20 min. After the reactant was completely dissolved, 3−4 drops of bromophenol blue reagent were added, and 0.1 mol/L HCl standard solution was used for titration. The titration end point was that the solution changed from blue to yellow. At the same time, a blank experiment was conducted. The value of the isocyanate value base can be calculated according to formula 1.

$$\mathrm{NCO\%} = \frac{(V_1 - V_2)\cdot c \times 4.2}{m} \quad (1)$$

where V_1 is the volume of hydrochloric acid standard solution consumed in the blank experiment (mL), V_2 is the volume of hydrochloric acid standard solution consumed by the sample (mL), C is the concentration of hydrochloric acid standard solution (mol/L), and m is the mass of the sample (g).

2.2. Monitoring of the Organosilicon Intermediate Reaction Process. In the process of preparing the organosilicon intermediate and modifying UV-curable epoxy acrylate, the change of NCO content in the reaction process was monitored by acetone di-*n*-butylamine titration and infrared measurement so as to determine whether the reaction reached the end point (Table 1).

Table 1. Change of −NCO Content during the Experiment

reaction time (min)	−NCO%
0	41.8
30	19.8
60	10.7

2.3. Characterization of Silicone-Modified EA. Figure 1 shows the synthesis of silicone intermediate products and the infrared spectrum curve of epoxy resin under silicone modification. It can be found from the figure that the absorption peak of −NCO appeared at 2270 cm^{-1} after 30 min of reaction by adding hydroxyl silicone oil (HSO) into IPDI, then the content of −NCO decreased significantly at 2270 cm^{-1} after adding HEA, and the absorption peaks of C═C and N−H appeared at 1670 and 3510 cm^{-1}, respectively, indicating that the reaction between −NCO and −OH was completed, and the C═C group was successfully introduced. After the above reaction is completed, EA is added to the synthesized organosilicon. It can be found from the figure that the characteristic absorption peak of −NCO at 2270 cm^{-1} disappears after the reaction with EA, and the peak of N−H exists at 3510 cm^{-1}, which indicates that −NCO reacts with −OH on the EA side chain, and the organosilicon group is successfully introduced into the EA side chain.

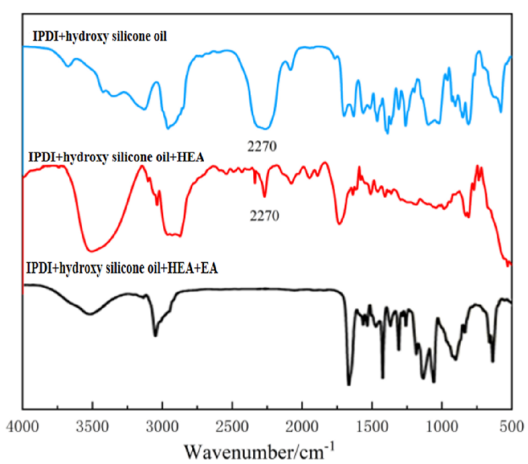

Figure 1. FT-IR spectrum of organosilicon-modified EA.

2.4. Effect on Curing Shrinkage of Photosensitive Resin with Different Contents of Silicone. Figure 2 shows the effect of different mole ratios of silicone to epoxy acrylate on the curing shrinkage of 3D printing UV curing resin. From the figure, it can be found that with the molar ratio of n(silicone):n(EA) increasing, the volume shrinkage and linear shrinkage of 3D printing photosensitive resin show a decreasing trend. When the ratio of n(silicone):n(EA) is more than 0.2:1, the curing shrinkage is basically kept below 6%, which meets the requirements of 3D printing curing. When the ratio is 0.5:1, the curing shrinkage reaches the minimum value of 4.57%. This is because in the curing process, the SLA-3D printing technology mainly uses the photochemical reaction. In addition to the shrinkage caused by the tight arrangement of atoms, there is also the change of free volume caused by the transformation from a monomer to a polymer during the curing process, and the monomer molecules are in a linearly loose active state before curing. After curing, the intermolecular crosslinking density increases, the movement of the chain segment is limited, and the free volume becomes smaller, resulting in larger shrinkage. The addition of silicone intermediate products can effectively improve this phenomenon, and the change of free volume before and after polymer curing is small so as to reduce the curing shrinkage of the system.

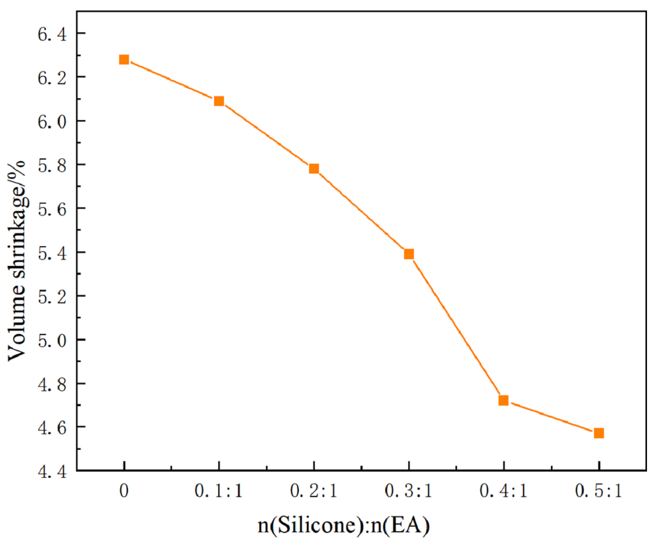

Figure 2. Effect of different n(silicone):n(EA) molar ratios on resin curing shrinkage.

2.5. Effect of Silicone Content on the VS of Photosensitive Resin. Figure 3 shows the effect of different mole ratios of silicone to epoxy acrylate on the VS of 3D printing UV curing resin. From the figure, it can be seen that the VS of 3D printing photosensitive material before curing increases with the increase in the molar ratio of silicone to

https://doi.org/10.1021/acsomega.3c02275
ACS Omega 2023, 8, 23044−23050

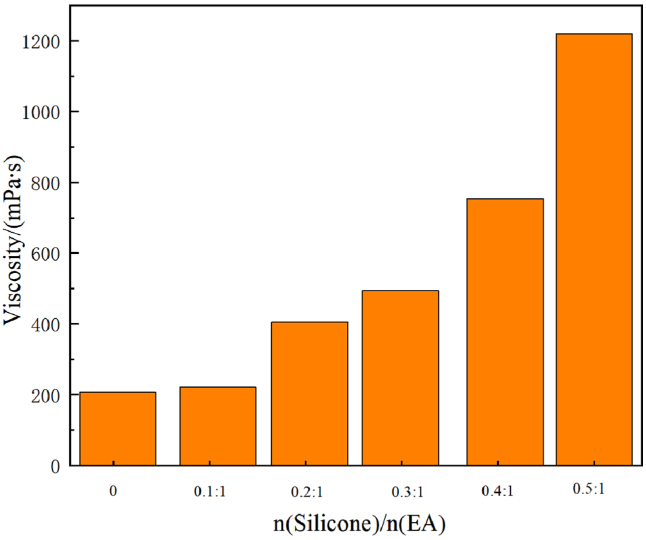

Figure 3. Effect of different n(silicone):n(EA) molar ratios on the VS of resin.

epoxy acrylate. When n(silicone):n(EA) is 0.5:1, the VS reaches 1320 MPa·s, which is 81.1% higher than that of pure epoxy resin. On the one hand, the product's increasing VS is due to the fact that HSO and IPDI undergo a polycondensation reaction in the process of the preparation of a silicone intermediate, resulting in the chain extension, which leads to the obvious increase in the molecular weight of the modified epoxy acrylate, resulting in the increase in VS. On the other hand, due to the poor compatibility between EA and silicone intermediates, there will be a certain degree of phase separation phenomenon, silicone intermediates contain an amino methyl ester acid bond, and the amino methyl ester acid bond will undergo hydrogen bonding, which makes the photosensitive resin's VS increase.

2.6. Influence of Organosilicon Content on Mechanical Properties of Photosensitive Resin. Figure 4 shows the effect of epoxy resin modified under different contents of organosilicon on the mechanical properties of the printing piece. From panels (a), (b), and (d), it can be seen that with the increase in n(silicone):n(EA) mole ratio, the TS of the modified printing piece decreases, and the IS and EAB are improved. It can be seen from panel (c) that with the increase in n(silicone):n(EA) mole ratio, the hardness value after addition is decreased compared with that without addition, but the influence is not great. The hardness value always changes in the range of 75−85 HD. When n(silicone):n(EA) =0.5:1, the IS increased from 14.6 to 19.4 kJ/m^2, 32.8% higher than

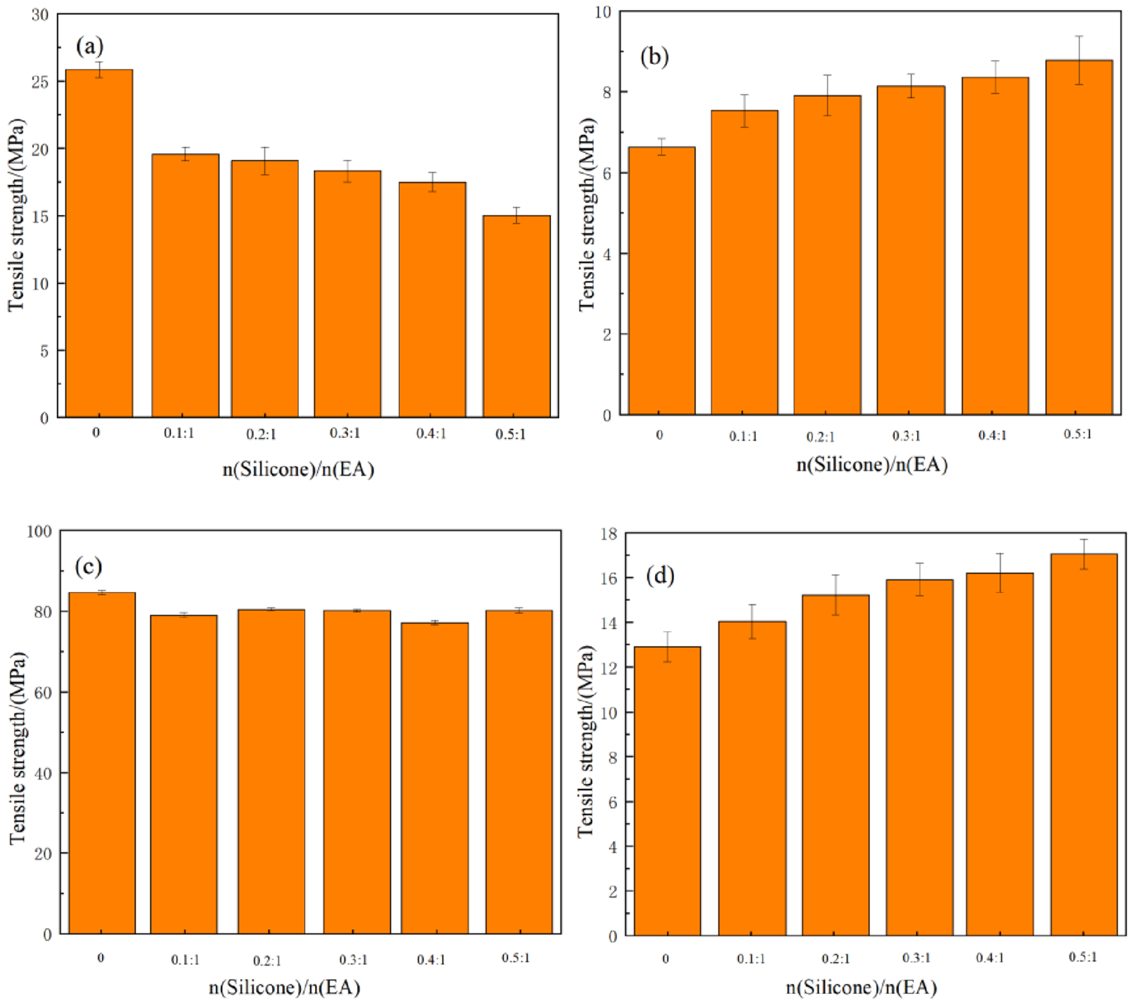

Figure 4. Effect of different contents of silicone-modified EA on the mechanical properties of molded parts: (a) TS, (b) EAB, (c) hardness, and (d) IS.

that without addition, and the EAB increased from 6.56 to 8.65%. The reason for the decrease in TS may be that the introduced flexible −Si−O− chain acts as a new network node in epoxy resin. With the increase in −Si−O− chain, the internal stress of epoxy resin is reduced, thus improving the toughness of printing parts.

2.7. Micromorphology Analysis of Tensile Section under Silicone-Modified Photosensitive Resin. Figure 5 shows the micromorphology of tensile section of the pure epoxy resin and silicone-modified epoxy resin with different molar ratios. From the comparison of micromorphology, it can be found that the tensile fracture surface is smooth under no modified resin, and the crack of cross section is thin and shallow, which is the embodiment of typical brittle fracture characteristics; however, the tensile fracture surface of the silicone-modified resin becomes rough, the folds of the fracture surface increase, the cracks become deeper, and obvious ductile depressions appear. The appearance of these characteristics indicates that the −Si−O− bond energy of silicone is much greater than the −C−C− bond energy and −C−O− bond energy, so the cured modified resin absorbs more energy than the unmodified resin; thus, the brittle fracture turns to a ductile fracture. Due to the addition of flexible −Si−O− segments, the proportion of rigid epoxy acrylate decreased, which played a toughening role to a certain extent. In addition, with the increase in silicone content, the silicone intermediate synthesized by IPDI, HSO, and HEA contains cyclohexane rigid groups. With the increase in silicone content, the rigid groups in the resin gradually increase, so the toughness of cured resin decreases.

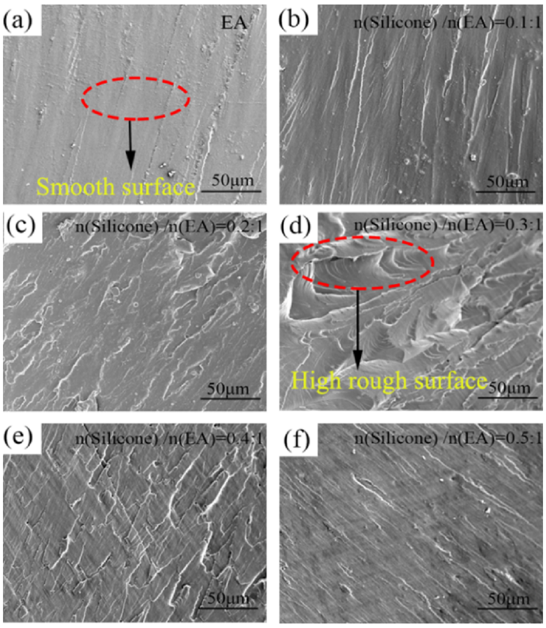

Figure 5. SEM images of the tensile fracture surface on different contents of silicone-modified epoxy resin: (a) pure EA, (b) n(silicone):n(EA) = 0.1:1, (c) n(silicone):n(EA) = 0.2:1, (d) n(silicone):n(EA) = 0.3:1, (e) n(silicone):n(EA) = 0.4:1, and (f) n(silicone):n(EA) = 0.5:1.

2.8. Thermal Weight Loss Curve of Organosilicon-Modified Photosensitive Resin. Figure 6 shows the thermal weight loss curves of pure epoxy resin and silicone modified by different proportions. Table 2 shows the corresponding data of $T_{50\%}$, T_{max}, and 800 °C residual masses. It can be found from the figure that the thermal stability of epoxy resin is improved after being modified by organosilicon. When n(silicone):n(EA) is 0.3:1, the $T_{50\%}$ and T_{max} of photosensitive resin are 1.9 and 6 °C higher than that of the epoxy resin before modification. The maximum temperature of thermal weightlessness is due to the silicone chain and double bond on the side link of epoxy acrylate. After heating, the silicone chain segment will decompose to form silica coating on the surface of epoxy resin to form a glass-like protective layer. Further decomposition of epoxy resin is hindered to some extent, thus improving the thermal stability of epoxy resin.

2.9. Effect of Silicone Modification on the GTT of Resin. GTT is one of the important indexes for resin to judge its heat resistance. To investigate the effect of silicone modification on GTT after printing and curing, DSC analysis was carried out on epoxy resin modified with different mole ratios. Figure 7 shows the GTT curve of silicone-modified epoxy resin. From the test results, it can be found that with the increase in silicone content in the system, and the GTT of modified epoxy resin first increases, then decreases, and reaches the maximum when the ratio of n(silicone):n(EA) is 0.4:1, which is 8.46 °C higher than that of unmodified epoxy resin. The reason is that the organic silicon intermediate contains −NH−, which easily forms a hydrogen bond, and the side chain contains a ring-shaped rigid group, which affects the free movement of the siloxane chain segment and improves the modified epoxy resins' GTT after curing.

3. CONCLUSIONS

(1) It can be seen by infrared characterization that a kind of intermediate organosilicon product was successfully prepared and epoxy acrylic resin was modified. The side link branch was a double bond of −Si−O− chain and carbon.

(2) The mechanical property test shows that silicone modification can improve mechanical properties of the epoxy resin. The IS and EAB of epoxy resin were improved after the modification of organosilicon, and the TS decreased to some extent. When the ratio of n(silicone):n(EA) is 0.3:1, the mechanical properties of the modified epoxy resin are better, the IS of the molding parts is increased from 14.6 to 19.4 kJ/m^2, 32.8% higher than that without addition of the epoxy resin, and the EAB increases from 6.56 to 8.65%.

(3) The results of TGA showed that the silicone-modified resin improved the heat resistance. When the ratio of n(silicone):n(EA) is 0.3:1, the $T_{50\%}$ and T_{max} of the modified resin are 1.9 and 6 °C higher than that of pure epoxy resin, and the heat resistance is improved. The DSC test shows that the glass conversion temperature of epoxy resin can be significantly increased by adding organosilicon. With the increase in organosilicon content, the glass conversion temperature increases first and then decreases. The maximum value is reached at 0.4:1, which is 8.46 °C higher than that before modification.

4. EXPERIMENTAL SECTION

4.1. SLA Process. The Moai SLA 3D printer was produced from Peopoly Company, Hong Kong, China, for photosensitive resin molding. For the setting parameters, the main

https://doi.org/10.1021/acsomega.3c02275
ACS Omega 2023, 8, 23044−23050

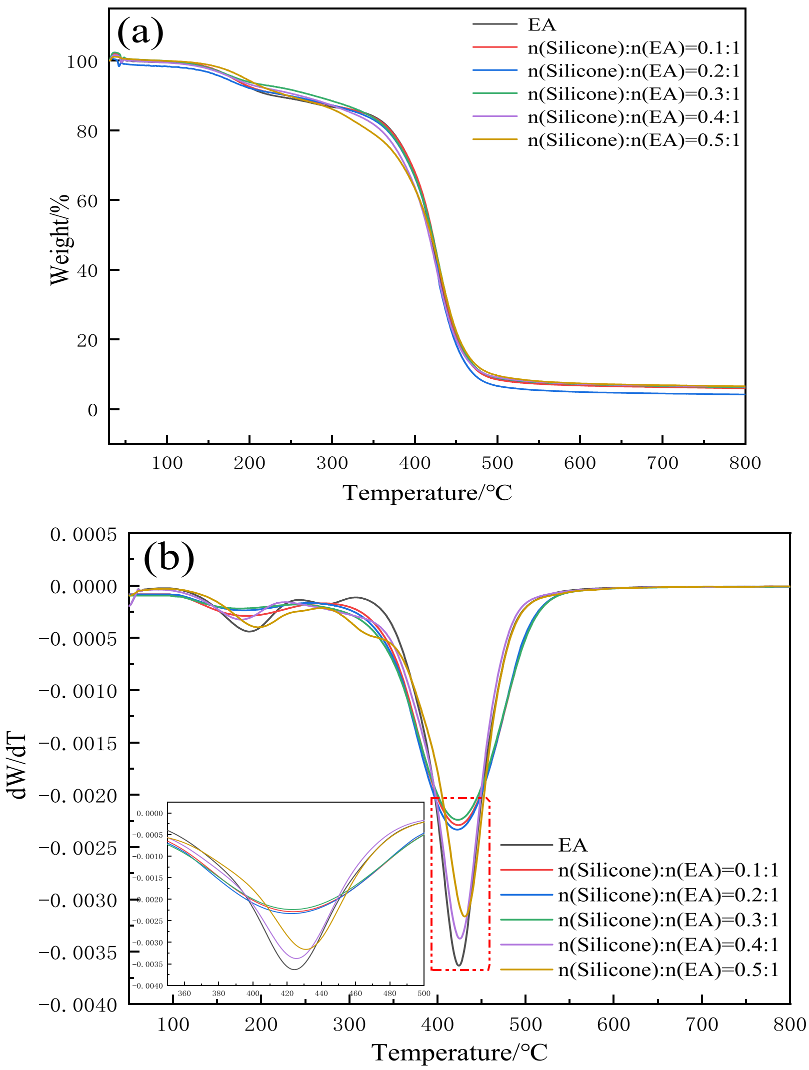

Figure 6. (a) TG and (b) DTG curves of organic silicon-modified 3D printing photosensitive material.

Table 2. Pure Epoxy Resin and Different Proportions of Silicone Modification

n(silicone):n(EA)	$T_{50\%}$ (°C)	T_{max} (°C)	residue (%)
0	421.89	424.33	8.3447
0.1:1	424.33	428.33	7.5148
0.2:1	424.78	427.67	5.5766
0.3:1	423.79	430.33	8.2051
0.4:1	419.23	424.33	8.0885
0.5:1	424.80	430.33	8.5411

emission wavelength is 405 nm, the layer thickness is 0.1 mm, the ultraviolet laser power is 58 W, and the printing speed is 40 mm/h.

4.2. Raw Materials. Bisphenol, an epoxy acrylate (EA), 1,6-hexanediol diacrylate (HDDA), tripropylene glycol diacrylate (TPGDA), trimethylolpropane triacrylate (TMPTA), 2,4,6-trimethylbenzoyl diphenylphosphine oxide (TPO), isophorone diisocyanate (IPDI), HSO, hydroxyethyl acrylate (HEA), dibutyltin dilaurate (dbtdl), hydroquinone acetone, dibutylamine, hydrochloric acid, and distilled water were used in this study.

4.3. Synthesis of the Organosilicon Intermediate. First, 0.2 mol (44.56 g) of isophorone diisocyanate (IPDI) was added into a three-port flask (spherical condenser, electric stirrer, and constant pressure separating funnel included), then the temperature of the solution was raised to 65 °C, 2−3 drops of dibutyltin dilaurate were added, and 0.1 mol (9.217 g) of

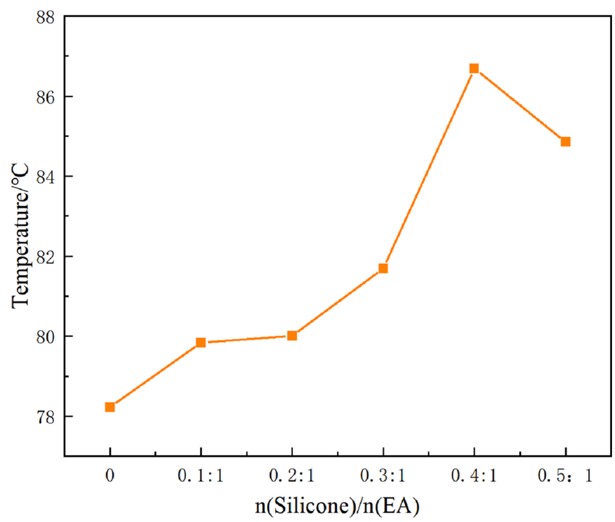

Figure 7. T_g change curves of silicone-modified epoxy resin.

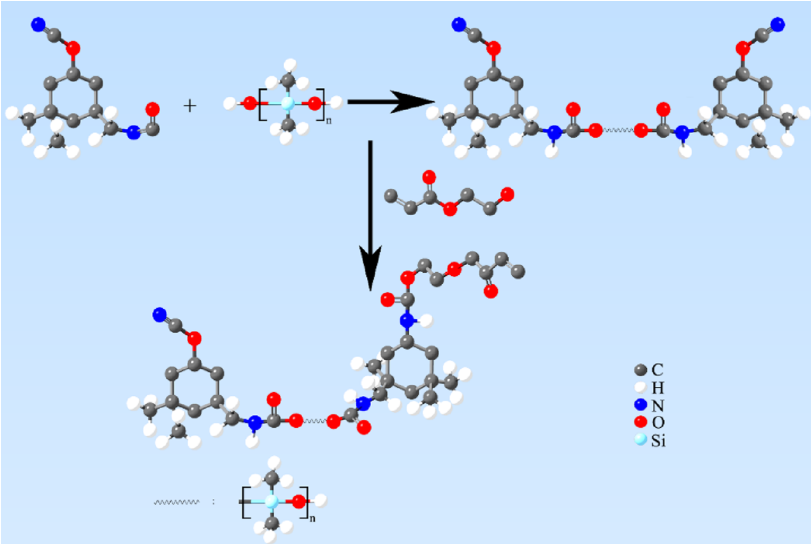

Figure 8. Synthesis mechanism of organosilicon intermediates.

hydroxy silicone oil was added into it (Figure 8). After the dropping, the content of −NCO with 0.1 mol/L acetone di-*n*-butylamine solution was measured every 10 min. Second, when the content of −NCO was reduced to half of the initial value, 0.1 mol (11.612 g) of hydroxyethyl acrylate (HEA) and an appropriate quantity of polymerization inhibitor hydroquinone were added. Finally, after the complete dropping, the content of −NCO in the solution was measured every 10 min; when the content of −NCO reached the theoretical value, the reaction was completed.

4.4. Synthesis of Silicone-Modified UV-Curable Epoxy Acrylate (EA). The intermediate product was cooled to room temperature, and acetone was added (Figure 9). Then, epoxy acrylate was added into a three-port flask and heated to 50 °C. The change of NCO content was monitored by acetone di-*n*-butylamine titration and infrared spectroscopy. When the absorption peak of −NCO at 2270 cm^{-1} on the infrared spectrum completely disappeared, the reaction reached the end point, and then acetone was distilled at atmospheric pressure.

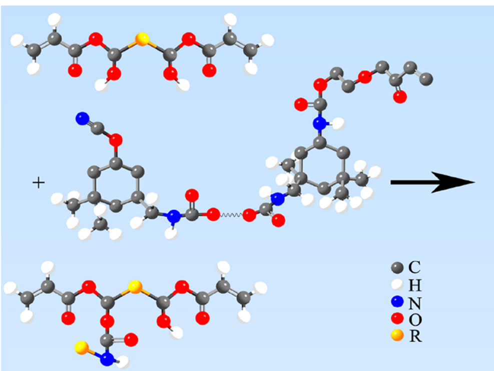

Figure 9. Synthesis mechanism of silicone-modified epoxy acrylate.

4.5. Preparation and Printing of Silicone-Modified UV Curing Resin. The prepared organosilicon and EA were reacted in different molar ratios (0.1:1, 0.2:1, 0.3:1, 0.4:1, and 0.5:1). After the reaction, the mixed solution of EA and HDDA with a mass ratio of 1.7 and a mass fraction of 4.5% photoinitiator was added. After that, the mixture was stirred by light proof magnetic force for 4 h, the rotation speed was 1000 rpm, and the mixture was kept for 12 h of 3D printing molding.

4.6. Photosensitive Resin SLA Rapid Prototyping. The silicone-modified 3D printing photosensitive resin material was printed by SLA equipment, and the resin-based parts with a complex structure were obtained. From Figure 10, it can be seen that the 3D printing resin grafted with the epoxy side chain by the organosilicon intermediate synthesized in the laboratory can be fully molded, which meets the performance requirements of SLA molding photosensitive resin. After molding, the surface of simple parts is smooth, the structure is complete, and there are no obvious defects and residual resin.

Figure 10. Resin-based molded parts.

AUTHOR INFORMATION

Corresponding Author

Yang Xiao − *School of Safety Science and Engineering, Xi'an University of Science and Technology, Xi'an 710054 Shaanxi, PR China; Shaanxi Key Laboratory of Prevention and Control of Coal Fire, Xi'an University of Science and Technology, Xi'an 710054, PR China;* orcid.org/0000-0002-3960-9708; Email: xiaoy@xust.edu.cn

Authors

Zhen-Guo Yan − *School of Safety Science and Engineering, Xi'an University of Science and Technology, Xi'an 710054 Shaanxi, PR China*

Zhen-Ping Wang − *School of Safety Science and Engineering, Xi'an University of Science and Technology, Xi'an 710054*

https://doi.org/10.1021/acsomega.3c02275
ACS Omega 2023, 8, 23044−23050

Shaanxi, PR China; Shaanxi Key Laboratory of Prevention and Control of Coal Fire, Xi'an University of Science and Technology, Xi'an 710054, PR China

Ying-Ying Liu − *School of Safety Science and Engineering, Xi'an University of Science and Technology, Xi'an 710054 Shaanxi, PR China*

Ning Yue − *Weilai Energy-chemical Co., Ltd., Jinjitan Coalmine, Yulin 719000 Shaanxi, PR China*

Complete contact information is available at: https://pubs.acs.org/10.1021/acsomega.3c02275

Notes

The authors declare no competing financial interest.

■ ACKNOWLEDGMENTS

The authors thank Professor Jin Chen for providing theoretical guidance for this work. They also thank Lei Ning for providing drawing support for this work.

■ REFERENCES

(1) Han, Z. Y.; Chang, C. Fabrication and Thermal Performance of a Polymer-Based Flexible Oscillating Heat Pipe via 3D Printing Technology. *Polymer* **2023**, *15*, 414−424.

(2) Li, Q. L.; Pan, Z. X.; Liang, J. J.; Zhang, Z. B.; Li, J. G.; Zhou, Y. Z.; Sun, X. F. Ceramic composites toughened by vat photopolymerization 3D printing technology. *J. Mater. Sci. Technol.* **2023**, *146*, 42−48.

(3) Chia, H. N.; Wu, B. M. Recent advances in 3D printing of biomaterials. *J. Biol. Eng.* **2015**, *9*, 1−14.

(4) Dong, D.; Su, H. J.; Li, X.; Fan, G. R.; Zhao, D.; Shen, Z. L.; Liu, Y.; Guo, Y. N.; Yang, C. B.; Liu, L.; Fu, H. Z. Microstructures and mechanical properties of biphasic calcium phosphate bioceramics fabricated by SLA 3D printing. *J. Manuf. Processes* **2022**, *81*, 433−443.

(5) Compton, B. G.; Lewis, J. A. 3D-printing of lightweight cellular composites. *Adv. Mater.* **2014**, *26*, 5930−5935.

(6) Espalin, D.; Muse, D. W.; MacDonald, E.; Wicker, R. B. 3D printing multi functionality: structures with electronics. *Int. J. Adv. Manuf. Technol.* **2014**, *72*, 963−978.

(7) Zadpoor, A. A.; Malda, J. Additive manufacturing of biomaterials, tissues, and organs. *Ann. Biomed. Eng.* **2017**, *45*, 1−11.

(8) Murphy, S. V.; Atala, A. 3D bioprinting of tissues and organs. *Nat. Biotechnol.* **2014**, *32*, 773−785.

(9) Keriquel, V.; Oliveira, H.; Rémy, M.; Ziane, S.; Delmond, S.; Rousseau, B.; Rey, S.; Catros, S.; Amédée, J.; Guillemot, F.; Fricain, J. In situ printing of mesenchymal stromal cells, by laser-assisted bioprinting, for in vivo bone regeneration applications. *Sci. Rep.* **2017**, *7*, 1−10.

(10) Banks, J. Adding value in additive manufacturing: researchers in the United Kingdom and Europe look to 3D printing for customization. *IEEE Pulse* **2013**, *4*, 22−26.

(11) Yue, J.; Zhao, P.; Gerasimov, J. Y.; van de Lagemaat, M.; Grotenhuis, A.; Rustema-Abbing, M.; van der Mei, H. C.; Busscher, H. J.; Herrmann, A.; Ren, Y. 3D-Printable antimicrobial composite resins. *Adv. Funct. Mater.* **2015**, *25*, 6756−6767.

(12) Gauvin, R.; Chen, Y. C.; Lee, J. W.; Pinar, Z.; Jason, W.; Hojae, B.; Chen, S.; Ali, K. Microfabrication of complex porous tissue engineering scaffolds using 3D projection stereolithograph. *Biomaterials* **2012**, *33*, 3824−3834.

(13) Zhou, T.; Zhang, L.; Yao, Y. L.; Ma, Y. L.; Hou, C.; Sun, B. H.; Shao, C.; Gao, P.; Chen, H. SLA 3D printing of high quality spine shaped β-TCP bioceramics for the hard tissue repair applications. *Ceram. Int.* **2020**, *46*, 7609−7614.

(14) Cui, M.; Zhang, L.; Lou, P.; Zhang, X. Z.; Han, X. J.; Zhang, Z. J.; Zhu, S. H. Study on thermal degradation mechanism of heat-resistant epoxy resin modified with carboranes. *Polym. Degrad. Stab.* **2020**, *176*, 109143.

(15) Yeasmin, F.; Mallik, A. K.; Chisty, A. H.; Robel, F. N.; Shahruzzaman, M.; Haque, P.; Rahman, M. M.; Hano, N.; Takafuji, M.; Ihara, H. Remarkable enhancement of thermal stability of epoxy resin through the incorporation of mesoporous silica micro-filler. *Heliyon* **2021**, *7*, No. e05959.

(16) Barkane, A.; Platnieks, O.; Jurinovs, M.; Gaidukovs, S. Thermal stability of UV-cured vegetable oil epoxidized acrylate-based polymer system for 3D printing application. *Polym. Degrad. Stab.* **2020**, *181*, 109347.

(17) Ke, H.; Zhao, L.; Zhang, X.; Qiao, Y.; Wang, G.; Wang, X. Performance of high-temperature thermosetting polyimide composites modified with thermoplastic polyimide. *Polym. Test.* **2020**, *90*, 106746.

(18) Fei, Y.; Xu, L. W. A Glimpse and Perspective of Current Organosilicon Chemistry from the View of Hydrosilylation and Synthesis of Silicon-Stereogenic Silanes. *Synlett* **2021**, *32*, 1281−1288.

(19) Mubarak, S.; Dhamodharan, D.; Kale, M. B. A novel approach to enhance mechanical and thermal properties of SLA 3D printed structure by incorporation of metal−metal oxide nanoparticles. *Nanomaterials* **2020**, *10*, 217.

(20) Al-Turaif, H. A. Effect of TiO_2 surface treatment on the mechanical properties of cured epoxy resin. *J. Coat. Technol. Res.* **2011**, *8*, 727.

(21) Mubarak, S.; Dhamodharan, D.; Divakaran, N.; Kale, M. B.; Senthil, T.; Wu, L.; Wang, J. Enhanced mechanical and thermal properties of stereolithography 3D printed structures by the effects of incorporated controllably annealed anatase TiO_2 nanoparticles. *Nanomaterials* **2020**, *10*, 79.

(22) Sangermano, M.; Messori, M.; Rizzoli, A.; Grassini, S. UV-cured epoxy coatings modified with perfluoropolyether-based materials. *Prog. Org. Coat.* **2010**, *68*, 323−327.

(23) Decker, C.; Viet, T. N. T.; Decker, D.; Weber-Koehl, E. UV-radiation curing of acrylate/epoxide systems. *Polymer* **2001**, *42*, 5531−5541.

(24) Sumiyoshi, T.; Schnabel, W.; Henne, A. Photolysis of acylphosphine oxides II: The influence of methyl substitution in benzoyldiphenylphosphine oxides. *J. Photochem.* **1986**, *32*, 119−129.

(25) Liu, P.; Gu, A.; Liang, G.; Guan, Q.; Yuan, L. Preparation and properties of novel high performance UV-curable epoxy acrylate/hyperbranched polysiloxane coatings. *Prog. Org. Coat.* **2012**, *74*, 142−150.

(26) Rosso, P.; Ye, L.; Friedrich, K.; Sprenger, S. A toughened epoxy resin by silica nanoparticle reinforcement. *J. Appl. Polym. Sci.* **2006**, *100*, 1849−1855.

(27) Ma, S.; Liu, W. Q.; Yu, D.; Wang, Z. F. Modification of epoxy resin with polyether-grafted-polysiloxane and epoxy-miscible polysiloxane particles. *Macromol. Res.* **2010**, *18*, 22−28.

(28) Zhang, K.; Shen, M. M.; Wu, K.; Liu, H. F.; Zhang, Y. K. Comparative study on flame retardancy and thermal degradation of phosphorus-and silicon-containing epoxy resin composites. *J. Polym. Res.* **2011**, *18*, 2061−2070.

(29) Garoushi, S.; Vallittu, P. K.; Watts, D. C.; Lassila, L. V. J. Effect of nanofiller fractions and temperature on polymerization shrinkage on glass fiber reinforced filling material. *Dent. Mater.* **2008**, *24*, 606−610.

(30) Zou, H.; Wu, S.; Shen, J. Polymer/silica nanocomposites: preparation, characterization, properties, and applications. *Chem. Rev.* **2008**, *108*, 3893−3957.

(31) Liu, Y.; Chen, J.; Ning, L.; Sun, J. K.; Zhao, K.; Liu, L. Preparation and properties of nano-TiO_2-modified photosensitive materials for 3D printing. *e-Polymers* **2022**, *22*, 686−695.

https://doi.org/10.1021/acsomega.3c02275
ACS Omega 2023, 8, 23044−23050